An investigation of axial strain's effect on the loss and refractive index of the hollow-core photonic band gap fiber

Haixia Liu, Xuexia Zhang, Xiaobin Xu, Fuyu Gao
School of Instrument Science and Optic-electronics Engineering, Beijing University of Aeronautics and Astronautics, Beijing 100191, China
*corresponding author: Liuhx08@buaa.edu.cn

Keywords:hollow core photonic band gap fiber,axial strain,loss,refractive index

Abstract. The response to axial strain of a hollow core photonic band gap fiber(HC-PBF) is investigated. The fiber is designed to operate at 1550*nm* which have shown to be highly dependent on the exact fiber structure. The relationship between axial strain and confinement loss as well as refractive index is calculated using full vector finite element method. An experimental platform is built to test the effects of axial strain on loss and refractive index, results show that the change rate of loss vs. axial strain is 10*(dB/km)/g*, and for refractive index is $12.71\times10^{-6}/g$. Analysis demonstretes that the axial strain has great influence on the loss and the refractive index of HC-PBF, which laid a foundation for HC-PBF optic sensing applications

1. Introduction

In 1999, hollow core photonic band gap fiber was manufactured successfully for the first time. Because of its special light-transporting principle the fiber drew a lot attention. Hollow core photonic band gap fiber is based on the principle of photonic band gap of light transmission which is different from the total reflection of light of ordinary optical fibers, and its special mechanism of light transmission enables the light transmit in low refractive index material of the air[1]. Besides, hollow core photonic band gap fibers can be manufactured with the un-doped silica materials. Comparing with conventional optical fibers, the hollow core photonic band gap fibers have a lot of advantages, such as the low nonlinear degree, low magnetic sensitivity, good temperature stability, and low radiation sensitivity[2]. Therefore the hollow core photonic band gap fiber has potential advantages in the fiber optic gyroscope, and it has been applied to the fiber optic gyroscope at home and abroad[3]. However, the core of the hollow core photonic band gap fiber is an air-hole defect with the air holes cladding around the center defect where the SiO2 wall is very thin, which results in the hollow core photonic band gap fiber is more sensitive to stress change. It requires a certain force in advance during the ring winding process of the fiber optic[4]. Therefore, it is important to clear the influence of the strain on the major characteristic parameters of the fiber, which is necessary for circling the fiber ring. The axial force is one of the main stresses for circling the HC-PBF ring, thus it is necessary to analyze the effect of axial force on HC-PBF.

Based on finite element method (FEM)[5], structure deformation, loss and refractive index was calculated under different axial strain[6]. Experimental platform was built to test the effects of axial strain on loss and refractive index. Both simulation and experimental results provide the data support for the use of hollow core photonic band gap fiber in fiber optic gyro, as well as in other communication sensing areas about the hollow core photonic band gap fibers.

2. Model and simulation

The simulation model is built based on 7 cell core hollow core photonic band gap fiber(HC-1550-02). The radius of coating layer is 125 um, cladding radius is 60 um, and the diameter of the fiber core air hole is 13.7 um. Figure 1 shows the scanning electron microscope (SEM) image of the hollow core photonic band gap fiber(HC-PBF).

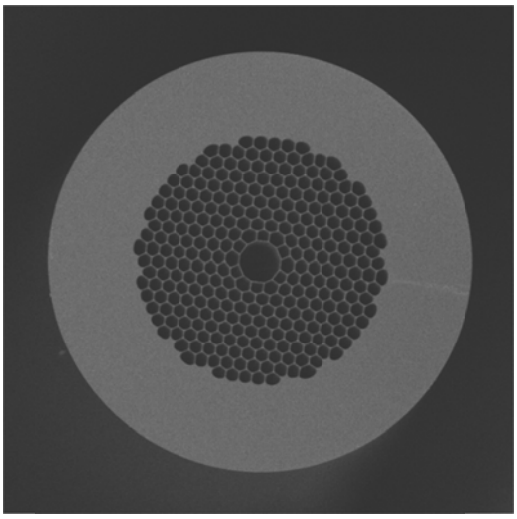

Figure 1 SEM image of the HC-PBF

The simulation model is built based on the interface structure obtained by the SEM image. 1/4 of the structure is selected as the study objects, as shown in figure 2. One of the interfaces of the hollow core photonic band gap fiber is fixed, and the uniform axial strain is applied on the other interface of the structure.

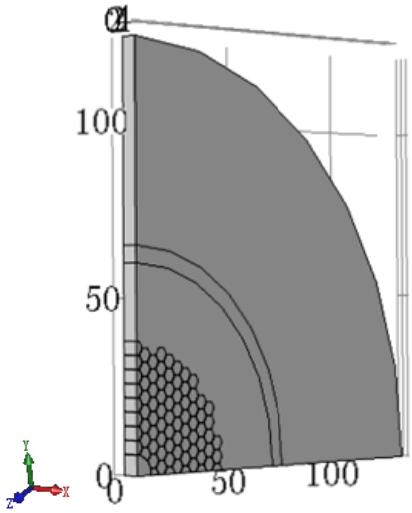

Figure 2 Three-dimensional structure model diagram of the HC-PBF

The cladding layer material of the HC-PBF is SiO2, whose Young's modulus is 72.45GP. The material of coating layer is acrylic resin, whose Young's modulus is only 0.5GP. When the axial strain acts on the end face of HC-PBF, the coating layer distorts more than the cladding layer. Therefore, the deformation at the interface of the coating layer and the cladding will larger than that at the core.

The displacement of the fiber end face is calculated with the axial strain changes from 5g to 50g, as shown in figure 3. Figure 3 shows that the displacement of the fiber core is almost zero. When the close to the coating layer (about 60μm to the central), the displacement is 2.1um at the strain of 50g, which is about 14 times that at the strain of 5g.

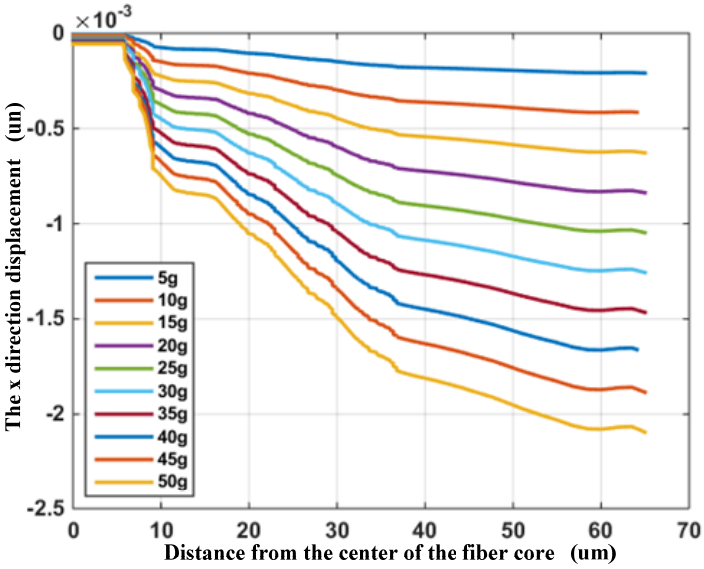

(a) The x direction displacement

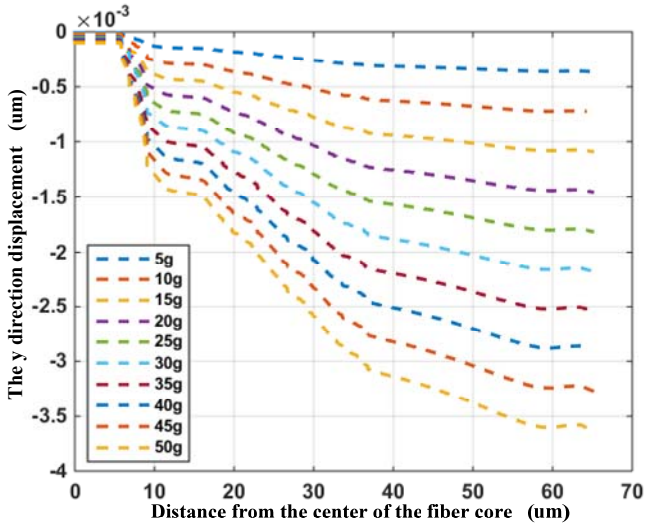

(b) The y direction displacement

Figure 3 X and Y direction of displacement relative to the fiber core center

2.1 Effects of the axial strain on confinement loss

The finite element methods transform Maxwell's equation into a characteristic equation to calculate the confinement loss of HC-PBF. By calculating the light field intensity distribution and propagation constant of the HC-PBF, it gets the confinement loss expressed by formula (1)[7]:

$$loss_c = -\frac{20\pi}{\ln 10} 10^6 \operatorname{Im}(\beta)(dB/m) \tag{1}$$

The $Im(\beta)$ is the imaginary part of the propagation constant.

By adding different axial strain, we could obtain a series of propagation constant values. Then the confinement loss under different axial strain is calculated according to equation (1), as shown in figure 4.

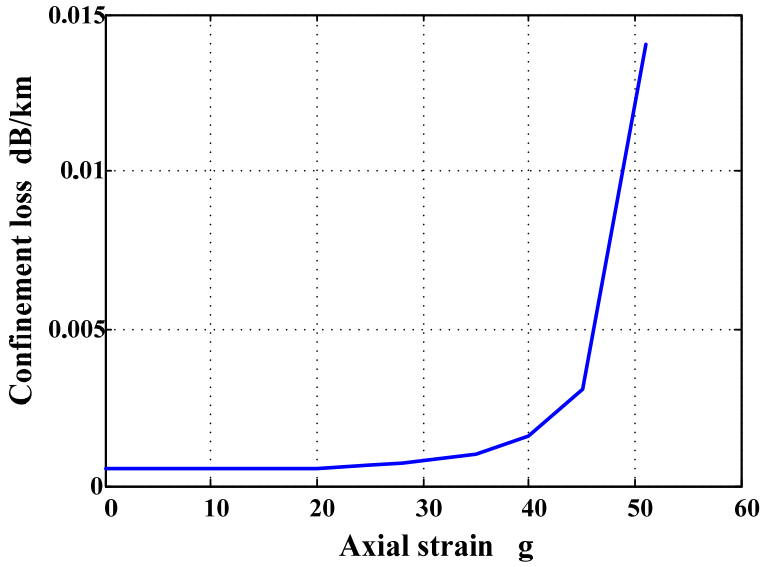

Figure 4 the confinement loss change along with the change of axial strain

Figure 4 show that when the axial strain is under 40g, the it has little influence on the confinement loss of the HC-PBF. However, the confinement loss increases rapidly when the axial strain goes up to 40g. Compared with figure 3, we could see that the increase of confinement is caused by the increase of displacement of the HC-PBF when the axial strain is larger than 40g.

2.2 Effects of the axial strain on refractive index

The propagation constant was calculated by solving the Maxwell's equation. With the real part of the propagation constant[8], the refractive index can be solved expressed as follows:

$$n_{eff} = \frac{\mathrm{Re}(\beta)}{k_0} \tag{2}$$

k_0 is the wave number in the vacuum, and n_{eff} is the refractive index of the HC-PBF.

From the above formula, the refractive index of the HC-PBF can be calculated through the propagation constant real part. When the axial strain acts on the HC-PBF the structure of the HC-PBF take place minimum displacement, which lead refractive index of the HC-PBF to change. With different axial strain values, a series of refractive index values was calculated. As is shown in figure 5, with the axial strain increasing, the refractive index of the HC-PBF changes greatly. And the rate of the refractive index is 0.02×10-6/g.

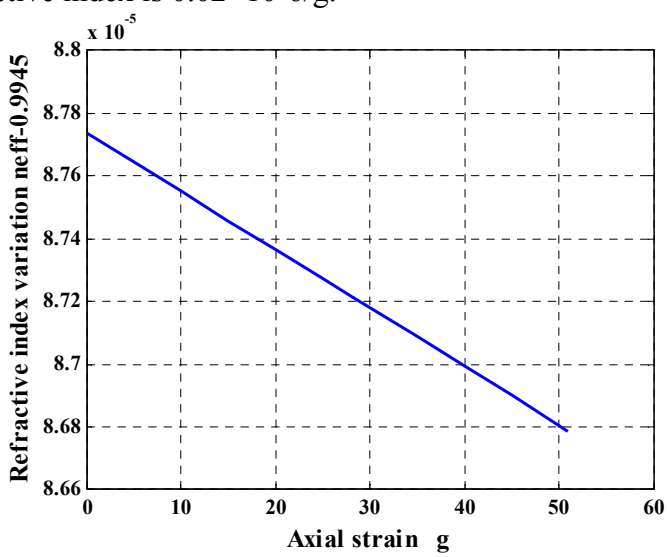

Figure 5 the change of refractive index along with the change of axial strain

3. Experiment

In order to verify the simulation results, experiments were carried out to test the variation of the loss and refractive index caused by the axial strain. The HC-PBF with a length of 1.7m was tested to analyze the influence of axial strain on the variation of loss. And the effect of axial strain on the variation of refractive index was analyzed by testing the HC-PBF with a length of 20cm. In the experiment, the two ends of the HC-PBF were connected with the light source and the power meter, separately. In order to test the variation of output power and refractive index under different axial strains, one end of the fiber is fixed, and the other end is put strain. The loss values of SMF under different axial strains were also tested for contrast and comparison with HC-PBF. Figure 6 gives the schematic diagram.

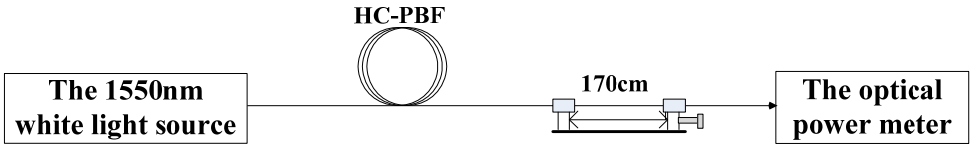

Figure 6

The principle diagram of the HC-PBF loss test

3.1 Influence of axial strain on the HC-PBF loss

The output power values were tested and recorded under different axial strains as well as under no axial strain. The loss of the HC-PBF can be calculated by formula (3)[9].

$$\alpha = \frac{10}{L}\log(\frac{P_{in}}{P_{out}})(dB/m) \tag{3}$$

P_{in} is the input optical power, and P_{out} is the output optical power. L represents the fiber length. Assume that the output optical powers under two different axial strains are P_1 and P_2, respectively. The loss variation between the two tests can be calculated by formula (4).

$$\Delta\alpha = \alpha_2 - \alpha_1 = \frac{10}{L}[\log(\frac{P_2}{P_1})] = \frac{10}{L}\log(\frac{P_2}{P_1}) \tag{4}$$

Figure 7 gives the experimental data and fitting curves of the loss variation of HC-PBF and SMF. It can be seen that, the loss variation is approximate to exponential growth with the axial strain increasing, and the maximal loss variation of the HC-PBF is about 10dB/km corresponding to a axial strain of 500g. However, the loss variation of SMF is almost unchanged in the range of 0~500 g axial strain. Both the simulation result and experimental result indicated that the loss of HC-PBF can be influenced by axial strain remarkably.

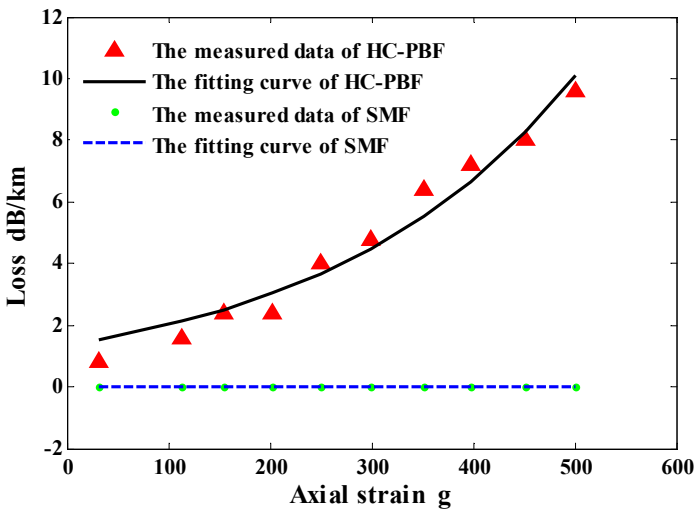

Figure 7 the axial strain effect on HC-PBF loss

3.2 Influence of the axial tension on HC-PBF refractive index

Based on the M-Z interference method[10] we designed the experiment to test the axial strain influence of the axial on the refractive index of the HC-PBF. The interference light field intensity is detected by the photoelectric detector. The schematic diagram is shown in Figure 8. We select the the laser light source at 1550*nm* and the photoelectric detector convert the light field intensity into a voltage value. The digital oscilloscope shows the voltage changes. According to the different numbers of voltage peak, The change of the optical path can be calculated. Therefore, the relationship between the change of the optical path and the axial strain can be obtained. As a comparison, the refractive index of traditional single mode fiber is measured.

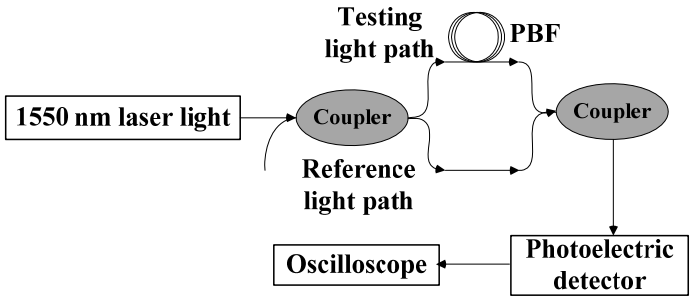

Figure 8 The principle diagram of the HC-PBF refractive index test

From the principle of figure 8, when the reference light path without change, $\Delta S'$ is the optical path difference between the two optical pass without stress.

$$\Delta S' = S_T - S_R \tag{5}$$

The length of HC-PBF fiber is L and its refractive index is n, the variation ΔS of the optical path difference is as the formula(6)：

$$\Delta S = \Delta S_T + S_T - \Delta S_R - \Delta S' = \Delta S_T = n \times L \tag{6}$$

In the process of the experiment, the HC-PBF will be elongated due to the applying axial strain on the HC-PBF, so both of the refractive index of the fiber and the fiber length would change. The optical path variation is:

$$\Delta S = n \times \Delta L + L \times \Delta n \tag{7}$$

The applying axial strain is F, the interface area of the fiber is S, the Principal stress of the fiber is σ, the Young's modulus is E, and the strain is ε. According to these formulas,

$$\sigma = \frac{F}{S} \tag{8}$$

$$\sigma = E \times \varepsilon \tag{9}$$

$$\varepsilon = \frac{\Delta L}{L} \tag{10}$$

$$\Delta n = \frac{\Delta S - n \times \Delta L}{L} \tag{11}$$

According to the experimental data, we can draw the figure 9. Because the optical path difference cannot be obtained accurately, so there will be a λ error within the experimental data. The red solid line is the fitting curve of the HC-PBF refractive index difference changes over the axial strain and the black fitting curve is the ordinary single-mode fiber refractive index difference changes with axial strain. By the tendency of the curve, HC-PBF is sensitive to stress more, whose rate of changing is $12.71 \times 10^{-6}/g$. Single mode optical fiber sensitivity to stress is weaker than

HC-PBF and its changing rate is $8.051\times10^{-6}/g$. Both of the two kinds of fiber refractive index difference is a linear change along with the changing stress.

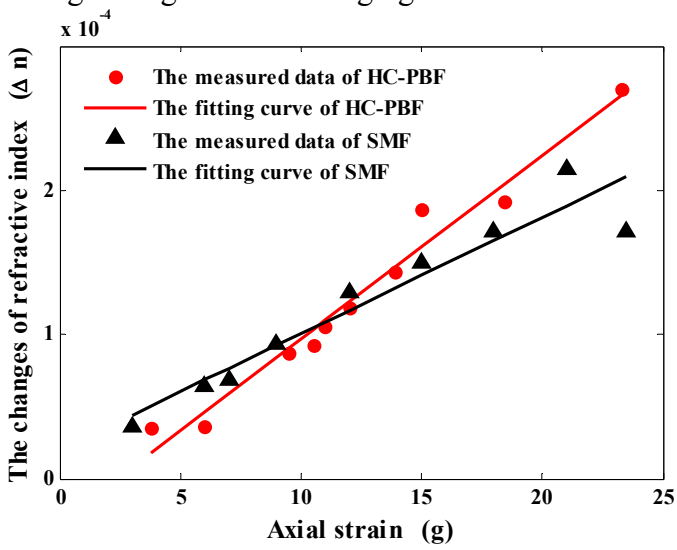

Fig 9 The optical path caused by axial strain

From the integrated simulation and experimental data, it can be concluded that the axial strain on the refractive index of the HC-PBF is more sensitive than single mode optical fiber. And the refractive index of the hollow core photonic band gap fiber has a linear proportional relationship with the axial strain.

4. Conclusion

Simulation and experimental results shows that axial strain of hollow core photonic band gap has great influence on the loss of the fiber, i.e. loss growth exponential with axial strain. Result provides the data support for fiber optic gyro applications. The refractive index of hollow core photonic band gap fiber is linearly proportional to axial strain, which laid the foundation for hollow core photonic band gap fibers used in axial strain sensor.

References

[1] Qu H, Ung B, Roze M, et al. All photonic bandgap fiber spectroscopic system for detection of refractive index changes in aqueous analytes[J]. Sensors and Actuators B: Chemical, 2012, 161(1): 235-243.

[2] Zubair A, Siddiqui S A, Alam M S. Birefringence and dispersion properties of elliptical hollow core optical fiber under hydrostatic pressure[C]//TENCON 2009-2009 IEEE Region 10 Conference. 2009.

[3] Pang M, Xiao L M, Jin W, et al. Birefringence of hybrid PCF and its sensitivity to strain and temperature[J]. Journal of Lightwave Technology, 2012, 30(10): 1422-1432.

[4] Sun Q, Mao Q, Liu E, et al. Hollow-core photonic crystal fiber high-pressure gas cell[C]//19th International Conference on Optical Fibre Sensors. International Society for Optics and Photonics, 2008: 700455-700455-4.

[5] Statkiewicz G, Martynkien T, Urbańczyk W. Measurements of birefringence and its sensitivity to hydrostatic pressure and elongation in photonic bandgap hollow core fiber with residual core ellipticity[J]. Optics communications, 2005, 255(4): 175-183.

[6] Van Vickle P S. Photonic Bandgap Fibers for Transverse Strain Sensing[M]. ProQuest, 2008.

[7] Pang M. Responses of photonic crystal fibres to pressure, axial strain and temperature[D]. The Hong Kong Polytechnic University, 2011.

[8] De Oliveira R E P, De Matos C J S. Response to pressure of a hollow core photonic crystal fiber for sensing applications[C]//Microwave and Optoelectronics Conference (IMOC), 2009 SBMO/IEEE MTT-S International. IEEE, 2009: 299-302.

[9] Kim G, Cho T, Hwang K, et al. Strain and temperature sensitivities of an elliptical hollow-core photonic bandgap fiber based on Sagnac interferometer[J]. Optics Express, 2009, 17(4): 2481-2486.

[10] de Oliveira R E P, de Matos C J S, Nunes G E, et al. Visible transmission windows in infrared hollow-core photonic bandgap fiber: characterization and response to pressure[J]. JOSA B, 2012, 29(5): 977-983.